The effect of joint translation constraint on within-participant variability of kinematics and kinetics during running in cerebral palsy

Chappell, A.; Liew, B.; Murphy, A. T.; Gibson, N.; Allison, G. T.; Williams, G.; Morris, S. L.

DOI:
10.1016/j.clinbiomech.2019.02.003

Document Version
Peer reviewed version

Citation for published version (Harvard):
Chappell, A, Liew, B, Murphy, AT, Gibson, N, Allison, GT, Williams, G & Morris, SL 2019, 'The effect of joint translation constraint on within-participant variability of kinematics and kinetics during running in cerebral palsy', *Clinical Biomechanics*, vol. 63, pp. 54-62. https://doi.org/10.1016/j.clinbiomech.2019.02.003

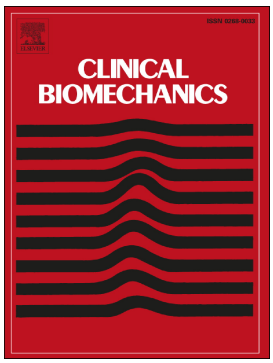

The effect of joint translation constraint on within-participant variability of kinematics and kinetics during running in cerebral palsy

A. Chappell, B. Liew, A.T. Murphy, N. Gibson, G.T. Allison, G. Williams, S.L. Morris

PII: S0268-0033(18)30878-7
DOI: https://doi.org/10.1016/j.clinbiomech.2019.02.003
Reference: JCLB 4689

To appear in: *Clinical Biomechanics*

Received date: 20 October 2018
Accepted date: 12 February 2019

Please cite this article as: A. Chappell, B. Liew, A.T. Murphy, et al., The effect of joint translation constraint on within-participant variability of kinematics and kinetics during running in cerebral palsy, Clinical Biomechanics, https://doi.org/10.1016/j.clinbiomech.2019.02.003

Original Article

The effect of joint translation constraint on within-participant variability of kinematics and kinetics during running in cerebral palsy

Chappell A[a], Liew B[a,b], Murphy AT[c,d], Gibson N[a,e], Allison GT[a], Williams G[f,g], and Morris SL[a]

Author main appointments and affiliations:

[a] School of Physiotherapy and Exercise Science, Curtin University, Perth, Western Australia, Australia. Email: annie.chappell@abilitycentre.com.au [b] Centre of Precision Rehabilitation for Spinal Pain (CPR Spine), School of Sport, Exercise and Rehabilitation Sciences, College of Life and Environmental Sciences, University of Birmingham, Birmingham, UK. Email LiewB@bham.ac.uk [c] Clinical Research Centre for Movement Disorders and Gait, Monash Health, Victoria, Australia [d] Faculty of Medicine, Nursing and Health Sciences, Monash University, Victoria, Australia Email: Anna.Murphy2@monashhealthorg [e] Perth Children's Hospital, Perth, Western Australia, Australia Email: noula.gibson@health.wa.gov.au [f] School of Health Sciences, University of Melbourne, Victoria, Australia [g] Epworth HealthCare, Victoria, Australia. Email: gavin.williams@epworth.org.au

Corresponding author:

Annie Chappell: Ability Centre, PO Box 61 Mt Lawley WA 6929 Australia fax: 08 9444 7299

email annie.chappell@abilitycentre.com.au

Word counts: Abstract = 229/250 Main Body=4006/4000

Abstract

Background Biomechanical data in cerebral palsy are inherently variable but no optimal model of translational joint constraint has been identified. The primary aim of this study was to determine which model of translational joint constraint resulted in the lowest within-participant variability of lower limb joint angles and moments. The secondary aim was to determine which model best distinguished known functional groups in Cerebral Palsy. *Methods* Three models (three degrees of freedom, six degrees of freedom and six degrees of freedom with specified joint translation constraint) were applied to data from running trials of 40 children with cerebral palsy. *Findings* Joint angle standard deviations were largest using the six degrees of freedom model and smallest using the constrained six degrees of freedom model (p<0.050). For all joints in all planes of motion, joint moment standard deviations were largest using the six degrees of freedom model and smallest using the constrained six degrees of freedom model; standard deviations using the constrained model were smaller than the three degrees of freedom model by 10-30% of moment magnitude (0.01 – 0.03 Nm/kg; p<0.001). The six degrees of freedom models distinguished functional subgroups with larger effect size than the three degrees of freedom model only for hip power generation in swing. *Interpretation* A model with specified joint constraint minimised within-participant variability during running and was useful for detecting differences in functional capacity in cerebral palsy.

Keywords: Biomechanics, Modelling, Gait, Kinematics, Kinetics

1. Introduction

Cerebral palsy is a term describing permanent but not unchanging disorders of movement and posture which result from an insult to the developing brain (Rosenbaum et al., 2007). Children with cerebral palsy are classified into five groups according to the Gross Motor Function Classification System (GMFCS) (Palisano et al., 2007). Children in GMFCS Level I are able to run, albeit with some

limitations, while about half the children in GMFCS level II are able to run, with more difficulty than those children in GMFCS level I (Böhm et al., 2018). Three-dimensional gait analysis is often undertaken to describe the effect of neuromuscular impairments or intervention on the gait of people with cerebral palsy (Böhm et al., 2018).

Kinematic and kinetic measurements generated by three dimensional gait analysis are inherently variable (Chia and Sangeux, 2017). Intrinsic variability is biological and represents flexibility of the neuro-motor system (Barrett et al., 2008). Intrinsic variability is higher in the cerebral palsy population compared to the typically developing population due to neuromotor impairments (Klejman et al., 2010; Steinwender et al., 2000). Extrinsic variability is introduced by the data collection and processing workflow and includes sources of error. The most significant sources of error are movement of skin markers with respect to the bone, termed soft tissue artefact, and the assumptions of the biomechanical model (Chia and Sangeux, 2017). Extrinsic variability in a data set may reduce statistical power which can result in a failure to detect true differences or changes (Sullivan and Feinn, 2012). This is a challenge for research in cerebral palsy, where sample sizes are often small, and the population is heterogeneous.

Inverse kinematics (IK) optimization is a technique proposed to reduce extrinsic variability by utilising modelled joint constraints (Leardini et al., 2005; Lu and O'connor, 1999), in which the position and orientation of the segment is calculated by minimizing the sum of squared displacements between the measured coordinates of all markers in the model and their modelled coordinates (Leardini et al., 2017). This is done according to the degrees of freedom (DoF) specified at each joint, termed joint constraints (Robinson et al., 2014). Joint constraint boundaries can be specified to mimic physiological joint limitations and can be derived directly from in-vivo methods or indirectly using data from published literature (Leardini et al., 2017). In a research study with many participants and many time points, it may not be considered feasible to employ individual

biomechanical models. A joint constraint model which can be applied to all participants at all time points may represent a significant efficiency, provided accuracy is maintained.

The magnitude of specified joint constraint impacts the variability of kinematic and kinetic gait measures (Kainz et al., 2016). For example, Potvin and colleagues (Potvin et al., 2017) reported a smaller standard deviation (SD) for knee rotation angle in the transverse plane during walking when knee joint constraints were informed from published in-vivo data, compared to a knee model with no constraints. A reduction in within-participant variation due to modelling implies a reduction in random error due to measurement, with the assumption that biological variability is maintained (Hopkins, 2000). The effect of specifying joint constraint boundaries at all modelled joints on the within-subject variability of kinematic and kinetic gait measures during running in people with cerebral palsy is unknown.

In intervention-based studies, such as in a Randomized Controlled Trial, less within-participant variability is desirable. For a given or difference in mean score of a biomechanical variable, smaller within-participant variability will result in greater effect size (Sullivan and Feinn, 2012). Consequently, a reduction in within-participant variability should increase the statistical power of a study and minimize the chance of falsely accepting the null hypothesis (Hopkins, 2000; Sullivan and Feinn, 2012).

The primary aim of this study was to determine which model of translational joint constraint: Model IK3 (3DoF); Model IK6 (6DoF) or Model IK6Constrained (specified joint translation constraint) resulted in the lowest within-participant variability of lower limb joint angles and moments. A biomechanical model which reduces within participant SD will be important for research and clinical use, as it represents a greater opportunity to detect an established known difference between different patient categories. The secondary aim of this study was to undertake a known groups analysis (Davidson, 2014) to identify which model/s were most effective at distinguishing known functional groups GMFCS level I and level II (Verschuren et al., 2010). By calculating effect sizes for

the different derived variables between children who are classified as GMFCS level I and those who are classified as GMFCS level II using each of the three models, we aim to determine whether any of the models separate the GMFCS levels, or 'known groups' with more statistical power than the others. If one of the models has larger effect sizes than the others, using this model in an intervention study may help to avoid a Type II error.

Methods

2.1 Participants

The present study represents the results of a sub-study from a larger project investigating the effects of a physical training program in children with cerebral palsy (Gibson et al., 2017). Data for the present study came from the three-dimensional running biomechanics collected at baseline prior to intervention. Forty-three children with cerebral palsy (aged 9 -18 years) with GMFCS level I-II and who were able to run independently were recruited (Gibson et al., 2017). Three participants were excluded from the present study due to the absence of a flight phase during running. A sample size of 40 provided us with 87% power to detect an effect size of 0.5 at an alpha value of 0.05 (G*Power v 3.1.9.2) (Faul et al., 2009). The study was approved by the Ethics Committees of Princess Margaret Hospital for Children, Perth, Western Australia (201405SEP) and Curtin University, Perth, Western Australia (HR 219/2014).

2.2 Data Collection

One experienced physiotherapist applied a modified Cleveland Clinic Foundation marker protocol (Sutherland, 2002) (Table 1). Participants wore their usual sport shoes and foot markers were placed on the shoes over the relevant landmarks. Participants were not allowed to use orthoses extending above the malleoli. Participants were asked to run at three speeds, 1) jog "like a warm-up", 2) run "faster but not your fastest", and 3) "sprint like you are in a race", along a 30m runway. At least five trials at each speed were collected unless the participant was too fatigued to continue. A two-minute sitting break was permitted between speeds if required. Kinematic data were recorded by an

18-camera motion capture system at 250Hz (Vicon T-series, Oxford Metrics, UK). Synchronized ground reaction forces were collected at 1000Hz using three in-ground force platforms in series (AMTI, Watertown, MA, USA). Marker trajectories were labelled and filled using Vicon Nexus 2.5 (Vicon Motion Systems, Oxford, UK).

2.2 Data processing

All data were processed using Visual 3D™ version 6 (C-Motion, Inc.). Kinematic and force plate data were filtered at 18 Hz using a zero-lag 4th order low-pass Butterworth filter following residual analysis (Yu et al., 1999). Three IK models were created from the same conditioned data, the only difference between models being the magnitude of the joint constraints applied (Table 2). All trials were processed using each of the three models described in Table 2. Model IK3 allowed 3DoF at each joint; flexion/extension, abduction/adduction and internal/external rotation with no translation permitted. Model IK6 allowed 6DoF without joint constraints; flexion/extension, abduction/adduction, internal/external rotation, medial/lateral translation, anterior/posterior translation and inferior/superior translation. Model IK6Constrained also allowed 6DoF but with specified joint translation constraints derived from the literature (Section 2.2.1).

2.2.1 Joint constraint parameters

Femoral head translation in healthy adults has been reported to be less than 4mm (Gilles et al., 2009). Children and adolescents with cerebral palsy GMFCS level I or II who are able to run, are at low risk of hip displacement (Kentish et al., 2011; Robin et al., 2009) but may have more hip joint translation than typically developing children (Kentish et al., 2011; Robin et al., 2009). Hence, 5mm of hip joint translation was permitted in model IK6Constrained (Table 2). There is less agreement in the research literature with respect to knee joint translation amplitude, but knee joint translation is consistently reported as greater in the anterior-posterior direction than medial-lateral direction in healthy adults (Sheehan et al., 2008), which was reflected in Model IK6Constrained (Table 2). There was diversity in reporting of ankle joint translations in healthy adults, including both the activity

(walking versus seated ankle plantarflexion/dorsifleixon) and the joints assessed (talocrural, talus relative to tibia or calcaneus relative to tibia) (de Asla et al., 2006; Imai et al., 2009; Sheehan et al., 2007). Ankle translations measured during walking (de Asla et al., 2006) were chosen for incorporation into Model IK6Constrained (Table 2) as data for running have not been reported.

2.2.2 Kinematics and Kinetics

For each model, pelvic segment angle, joint angles for hip, knee and ankle and net internal joint moments for the hip, knee and ankle were calculated for each trial in three planes (sagittal, frontal and transverse) and time normalized to 101 points from initial contact to initial contact of the same limb. For ankle, knee and hip joint angles an X-Y-Z (flexion-extension, abduction-adduction, internal-external rotation) cardan sequence was used, whilst for the pelvic segment angle a Z-Y-X sequence was used (Baker, 2001; Cole et al., 1993). Inertial and geometric properties of the segments were based on previously published models (Dempster, 1955; Hanavan Jr, 1964). A regression equation was used to calculate hip joint centres (Bell et al., 1989). Knee and ankle (talocrural) joint centres were calculated using the proximal joint centre and the midpoint between the medial and lateral femoral condyles, and malleoli respectively. Joint centres were located on the proximal end of the distal segment. The inferior-superior axis of each segment coordinate system lay along a vector connecting the joint centres. Each segment coordinate system was created using the anatomical plane and defined joint centres (O'Connor and Bottum, 2009; Palmieri-Smith et al., 2009).

Joint moments were resolved in the coordinate system of the proximal segment (Williams et al., 2004). Force plate threshold was set at 20N with foot on and foot off detected automatically. Gait events occurring off the force plates were automatically detected based on the axial and anteroposterior position of the proximal end of the foot for initial contact and the distal end of the foot for toe-off (Stanhope et al., 1990).

2.2.3 Within-participant, within-session variability

Data were grouped by speed (jog, run, sprint) and the between-trial standard deviations (SDs) calculated for each data point for each participant at each of the three running speeds for each of the three models (Kainz et al., 2017). The average SD across the gait cycle for each joint angle and moment was retained as a dependent variable (n=42 for each model at each speed for each subject).

2.3 Statistical Analysis

2.3.1 Within-participant variability

Natural log transformations were performed on joint angle SDs to correct right skewedness. Joint moment data were separated into stance and swing phases as these data were quite distinct. Two-step transformations to normality using the inverse distribution function were performed on stance and swing joint moment SDs to correct right skewedness. The transformed data were then analyzed in Statistical Analysis Software version 9.4 (SAS Institute Inc., Cary, NC, USA) using linear mixed models with fixed effects joint, model and gait phase (stance or swing) and random effects subject and speed. Interactions between fixed effects were excluded when not significant with alpha set at 0.05. Covariances were modelled as compound symmetry.

2.3.2 Known Groups Analysis

Known groups analysis was undertaken with participants classified as GMFCS level I or GMFCS level II. Derived variables considered pertinent to running were included; peak ankle, knee and hip power absorption in stance phase (A1, K1 and H2 respectively), peak ankle, knee and hip power generation in stance phase (A2, K2 and H1 respectively) and peak hip power generation in swing phase (H3). Spatiotemporal variables were not included as these were not expected to change depending on the IK model. Hedges g was calculated for all variables for the three models. Hedge's g is the most appropriate measure of effect size where sample size is less than 20 and the two sample sizes are different (Lakens, 2013). Hedge's g was thus considered most appropriate for this analysis of GMFCS level I (n=25) and GMFCS level II (n=15).

3 RESULTS

3.1 Participants

Forty-three participants were recruited to the study. Three were excluded from the analysis due to the absence of a flight phase. Participants were aged 12.69 years (SD=2.7 years); 25 males and 15 females; 25 GMFCS level I and 15 GMFCS level II; 21 bilateral cerebral palsy and 19 unilateral cerebral palsy. Two participants completed jog trials only. Three participants completed jog and run trials only. Of those who completed sprint trials, 13 completed three sprint trials, 14 completed four sprint trials and 8 completed five or more sprint trials.

3.2 Model performance

The IK6 and IK6C joint translations are reported in Table 2. The unconstrained 6DoF model resulted in larger joint translations than the constrained 6DoF model, especially at the hip.

3.3 Joint Angles

In general, the IK6 model resulted in the largest joint angle SDs and the IK6Constrained model resulted in the smallest joint angle SDs. The model applied only influenced pelvis segment angle in the frontal plane where both IK3 SDs and IK6Constrained SDs were 1.1^{o} smaller than IK6 SDs (p<0.001 and p<0.001) (Figures 1 and 2). At the hip, IK6Constrained SDs were 0.6^{o} smaller than IK3 SDs in the sagittal plane (p=0.003) and 0.7^{o} smaller in the transverse plane (p<0.001), but not different in the frontal plane (p=0.425). IK3 SDs were smaller than IK6 SDs in all planes (sagittal p=0.026, frontal p<0.001 and transverse p<0.001) (Figure 1). At the knee, IK6Constrained SDs were 0.2^{o} smaller than IK3 SDs in the frontal (p=0.038) transverse planes (p<0.001), but not different in the sagittal plane (p=0.393). IK3 SDs were smaller than IK6 SDs in all planes (sagittal p<0.001, frontal p<0.001 and transverse p<0.001) (Figure 1). At the ankle, IK6Constrained SDs were 0.1^{o} smaller than IK3 SDs in the frontal plane (p=0.038) and 0.5^{o} smaller in the transverse plane (p<0.001), but not different in the sagittal plane (p=0.216). IK3 SDs were smaller than IK6 SDs in the sagittal plane

(p<0.001) but not different in the transverse plane (p=0.725). In the frontal plane there was no difference between IK6Constrained and IK6 (p=0.135) or IK6 and IK3 (p=0.558) (Figures 1 and 2).

3.3 Joint Moments

For all joints in all planes of motion, IK6Constrained SDs were smaller than IK3 by 10-30% (0.01 – 0.03 Nm/kg (p<0.001 for each joint in each plane)) and IK3 SDs smaller than IK6 by 22-33% (0.03 – 0.13 Nm/kg (p<0.001 for each joint in each plane)) (Figures 2 and 3).

3.4 Speed

Speed (jog/run/sprint) did not have a significant effect in the linear mixed models.

3.5 Hedges g Effect Sizes

Large effect sizes (g>0.8) were found for A1, A2 and H2 for all IK models. Medium effect sizes (0.5>g<0.8) were found for K2 and H1 for all IK models. Small effect sizes (0.2>g<0.5) were found for K1 for all IK models. For H3, effect size was small for model IK3 (0.48) and medium for IK6 (0.58) and IK6Constrained (0.72)(Figure 4).

DISCUSSION

The main finding of this study was that specified joint constraint boundaries resulted in small but significant reductions in within-participant variability of estimated joint angles and moments at the ankle, knee and hip compared to the IK3 and IK6 models. The second main finding was that specified joint constraint boundaries resulted in a larger effect size when separating GMFCS levels I and II for hip power generation in swing, compared to the other two models.

Kinematic and Kinetic Variability

Extrinsic variability is introduced to a data set through the data collection and processing workflow and includes sources of error (Chia and Sangeux, 2017). Large amounts of extrinsic variability reduce statistical power and make it more difficult to identify true differences between groups, or between

time points in a given population (Hopkins, 2000). In this study, only the joint constraint boundaries were manipulated, so any reduction in variability can be confidently attributed to a reduction in extrinsic variability, which is desirable. Reducing extrinsic variability increases the likelihood of identifying true differences between groups or changes over time due to natural progression or intervention.

Overall, the IK6 model resulted in the greatest within-participant variability in both kinematics and kinetics. In a six DoF joint model, soft tissue artefact can result in overestimation of joint translation including apparent joint dislocations (Kainz et al., 2016; Leardini et al., 2005; Ojeda et al., 2016), which may explain the greater extrinsic variability. Compared to the IK3 model, the IK6Constrained model resulted in smaller within-participant variability for all joint moments, for joint angles in the transverse plane and knee joint angle in the frontal plane. Constraining a joint to three DoF can potentially mitigate soft tissue artefact by removing joint centre translation (Leardini et al., 2017), however assuming adjacent segments are pinned together also introduces error (Schmitz et al., 2016). Utilising joint constraint boundaries to allow restricted joint centre translation may explain why the IK6Constrained model resulted in lower variability than both the IK3 model and the IK6 model. This explanation is consistent with the findings of Potvin and colleagues (Potvin et al., 2017), who reported a smaller range of knee rotation using five DoF with bone-pin informed constraint compared to using five DoF without informed joint constraint boundaries in walking in healthy adults. The finding is important because both running gait and cerebral palsy are associated with high intrinsic variability (Estep et al., 2016; Klejman et al., 2010; Steinwender et al., 2000) and it has traditionally been difficult to recruit large numbers to studies in this population due to the heterogeneity of their clinical presentation. Minimising extrinsic variability is therefore important to improve statistical power in research studies in this population.

At the ankle, our IK3 joint angle SDs were similar or smaller in the sagittal and transverse planes to those reported using a three DoF model in healthy adult walking (Charlton et al., 2004; Schmitz et

al., 2016), but larger in the frontal plane than those reported in healthy adults walking (Charlton et al., 2004) or running (Hamacher et al., 2016) and larger than those reported in chronically unstable ankles while running (Hamacher et al., 2016). As the ankle joint complex consists of both the talo-crural joint and the subtalar joint, modelling it as a single joint is less realistic and therefore increases error in estimation of the position and orientation of the segment (Leardini et al., 2017). This may be magnified in children with cerebral palsy in whom ankle malalignment, instability and spasticity may all increase multi-planar movements at the ankle complex (Davids, 2010). Our medio-lateral ankle joint translation boundaries were based on healthy adult data as this was the most relevant data available. These boundaries may have been too restrictive, resulting in increased error.

Our IK6Constrained model resulted in joint moment SDs 0.02-0.03Nm/kg smaller than the IK3 model, which equates to a change of 10-30% of moment magnitude. Allowing a constrained amount of joint translation may permit the joint centre to be more accurately located during kinetic calculations, thereby reducing extrinsic variability. Joint moment SDs were larger than previously published studies of walking in healthy participants using three DoF joint models (Sangeux et al., 2016; Wong et al., 2010) but this is not surprising given joint moments are larger and more variable in running compared to walking (Estep et al., 2016; Novacheck, 1998), and more variable in children with cerebral palsy than typically developing children (Klejman et al., 2010; Steinwender et al., 2000). Potvin and colleagues (Potvin et al., 2017) reported a smaller effect of joint model DoF on joint moments compared to joint angles in walking, whereas the present study has found a significant reduction in all joint moment SDs using the IK6Constrained model. This may be because the IK6Constrained model incorporates joint constraint boundaries at all three lower limb joints, whereas Potvin and colleagues only specified joint constraint boundaries at the knee (Potvin et al., 2017). The effect of reducing error by using the IK6Constrained model may also have a magnified effect on force calculations due to the greater forces associated with running compared with walking (Smale et al., 2017).

From a clinical perspective, the effect of specified joint translation constraint on kinetics is perhaps more meaningful than the effect on kinematics (McGinley et al., 2009). For example, ankle push-off plantarflexor moment in this cohort ranges from 1 Nm/Kg during jogging to 3.5 Nm/Kg during sprinting. A reduction in SD of 0.1 Nm/kg in ankle push-off therefore equates to up to 10% reduction during a critical phase for forward propulsion. As the magnitude of clinically significant differences are yet to be defined, it is important to select the most sensitive methods available in both the research and clinical settings (Allison and Fukushima, 2003).

Effect Sizes

In the known groups analysis all three models had medium-to-large effect sizes when discriminating between GMFCS level I and II for peak power absorption and generation in stance phase, except for power absorption at the knee, which had a small effect size for all three models. The notable exception was for hip power generation in swing phase, where the IK3 model had a small effect size and both IK6 and IK6Constrained models had a medium effect size. This may mean that for research questions relating to the swing phase of running, six DoF models provide a larger effect size in a group-by-time interaction. Therefore, the number of participants required to be recruited will be less using a six DoF model. During swing phase of running the hip is moved rapidly through a large arc of movement (Novacheck, 1998) and thus is subject to high levels of soft tissue artefact (Peters et al., 2010). The application of joint constraints is one potential method to reduce the effect of soft tissue artefact but is dependent on the joint constraints specified (Leardini et al., 2017; Potvin et al., 2017). Our findings suggest that applying joint translation constraints appropriate for children with cerebral palsy can reduce the effect of measurement error on skeletal movement. The ability to generalise these findings across different diagnostic groups mediated by the phase of running may warrant further research.

Limitations

The main limitation of this study is that we did not have a gold standard with which to evaluate the accuracy of the three models, thus the mechanism by which joint translation constraint reduces within-participant variability cannot be determined. However, using bone-pins in this population is invasive and difficult to justify. Calculation of marker residuals and knee joint kinematic cross-talk would add to our understanding of the accuracy of a 6DoF model with specified joint constraints but was beyond the scope of this paper. This field remains an avenue for further research.

The joint constraint boundaries used in the present study were extracted from the research literature, rather than subject-specific in-vivo measures. The boundaries were applied to all subjects, as this may be preferable in a study with many participants and many time points. In clinical gait analysis when the individual is the focus, joint constraint boundaries which consider individual variations in bony geometry, ligamentous laxity and muscle length may be preferred (Lenaerts et al., 2008; Smale et al., 2017). However, there will be situations where time or resources exclude the possibility of individual modelling. In these circumstances, a 6DoF model with prescribed joint boundaries may be considered.

Conclusion

The application of specified joint constraint boundaries to an IK model reduces within-participant variability of kinetic and kinematic data during running in children and adolescents with cerebral palsy and results in greater sensitivity in the detection of between-group differences, particularly in the swing phase of running.

Conflict of Interest Statement

The authors declare no conflict of interest.

Acknowledgments and Funding

Annie Chappell is supported by an Australian Government Research Training Program Scholarship. Data processing was supported by a Perth Children's Hospital Foundation Grant ID 9632.

References

Allison, G.T., Fukushima, S., 2003. Estimating three-dimensional spinal repositioning error: the impact of range, posture, and number of trials. Spine (Phila Pa 1976) 28, 2510-2516.
Baker, R., 2001. Pelvic angles: a mathematically rigorous definition which is consistent with a conventional clinical understanding of the terms. Gait Posture 13, 1-6.
Barrett, R., Noordegraaf, M.V., Morrison, S., 2008. Gender differences in the variability of lower extremity kinematics during treadmill locomotion. Journal of motor behavior 40, 62-70.
Bell, A.L., Brand, R.A., Pedersen, D.R., 1989. Prediction of hip joint centre location from external landmarks. Hum Mov Sci 8, 3-16.
Böhm, H., Wanner, P., Rethwilm, R., Döderlein, L., 2018. Prevalence and predictors for the ability to run in children and adolescents with cerebral palsy. Clinical Biomechanics 58, 103-108.
Charlton, I., Tate, P., Smyth, P., Roren, L., 2004. Repeatability of an optimised lower body model. Gait & Posture 20, 213-221.
Chia, K., Sangeux, M., 2017. Quantifying sources of variability in gait analysis. Gait Posture 56, 68-75.
Cole, G., Nigg, B., Ronsky, J., Yeadon, M., 1993. Application of the joint coordinate system to three-dimensional joint attitude and movement representation: a standardization proposal. J. Biomech. Eng. 115, 344-349.
Davids, J.R., 2010. The foot and ankle in cerebral palsy. Orthop. Clin. North Am. 41, 579-593.
Davidson, M., 2014. Known-Groups Validity, in: Michalos, A.C. (Ed.), Encyclopedia of Quality of Life and Well-Being Research. Springer Netherlands, Dordrecht, pp. 3481-3482.
de Asla, R.J., Wan, L., Rubash, H.E., Li, G., 2006. Six DOF in vivo kinematics of the ankle joint complex: Application of a combined dual-orthogonal fluoroscopic and magnetic resonance imaging technique. J. Orthop. Res. 24, 1019-1027.
Dempster, W.T., 1955. Space requirements of the seated operator: geometrical, kinematic, and mechanical aspects of the body, with special reference to the limbs.
Estep, A., Morrison, S., Caswell, S., Ambegaonkar, J., Cortes, N., 2016. Differences In The Pattern Of Variability For Lower Extremity Kinematics Between Walking And Running.: 3845 Board# 284 June 4, 8: 00 AM-9: 30 AM. Med. Sci. Sports Exerc. 48, 1080.
Faul, F., Erdfelder, E., Buchner, A., Lang, A.-G., 2009. Statistical power analyses using G* Power 3.1: Tests for correlation and regression analyses. Behav. Res. Methods 41, 1149-1160.
Gibson, N., Chappell, A., Blackmore, A.M., Morris, S., Williams, G., Bear, N., Allison, G., 2017. The effect of a running intervention on running ability and participation in children with cerebral palsy: a randomized controlled trial. Disabil. Rehabil., 1-9.
Gilles, B., Christophe, F.K., Magnenat-Thalmann, N., Becker, C.D., Duc, S.R., Menetrey, J., Hoffmeyer, P., 2009. MRI-based assessment of hip joint translations. J. Biomech. 42, 1201-1205.
Hamacher, D., Hollander, K., Zech, A., 2016. Effects of ankle instability on running gait ankle angles and its variability in young adults. Clinical Biomechanics 33, 73-78.
Hanavan Jr, E.P., 1964. A mathematical model of the human body. AIR FORCE AEROSPACE MEDICAL RESEARCH LAB WRIGHT-PATTERSON AFB OH.
Hopkins, W.G., 2000. Measures of reliability in sports medicine and science. Sports Med 30, 1-15.
Imai, K., Tokunaga, D., Takatori, R., Ikoma, K., Maki, M., Ohkawa, H., Ogura, A., Tsuji, Y., Inoue, N., Kubo, T., 2009. In vivo three-dimensional analysis of hindfoot kinematics. Foot Ankle Int. 30, 1094-1100.
Kainz, H., Graham, D., Edwards, J., Walsh, H.P., Maine, S., Boyd, R.N., Lloyd, D.G., Modenese, L., Carty, C.P., 2017. Reliability of four models for clinical gait analysis. Gait Posture 54, 325-331.
Kainz, H., Modenese, L., Lloyd, D., Maine, S., Walsh, H., Carty, C., 2016. Joint kinematic calculation based on clinical direct kinematic versus inverse kinematic gait models. J. Biomech. 49, 1658-1669.
Kentish, M., Wynter, M., Snape, N., Boyd, R., 2011. Five-year outcome of state-wide hip surveillance of children and adolescents with cerebral palsy. J. Pediatr. Rehabil. Med. 4, 205-217.

Klejman, S., Andrysek, J., Dupuis, A., Wright, V., 2010. Test-retest reliability of discrete gait parameters in children with cerebral palsy. Arch. Phys. Med. Rehabil. 91, 781-787.
Lakens, D., 2013. Calculating and reporting effect sizes to facilitate cumulative science: a practical primer for t-tests and ANOVAs. Front. Psychol. 4, 863.
Leardini, A., Belvedere, C., Nardini, F., Sancisi, N., Conconi, M., Parenti-Castelli, V., 2017. Kinematic models of lower limb joints for musculo-skeletal modelling and optimization in gait analysis. J. Biomech.
Leardini, A., Chiari, L., Della Croce, U., Cappozzo, A., 2005. Human movement analysis using stereophotogrammetry: Part 3. Soft tissue artifact assessment and compensation. Gait Posture 21, 212-225.
Lenaerts, G., De Groote, F., Demeulenaere, B., Mulier, M., Van der Perre, G., Spaepen, A., Jonkers, I., 2008. Subject-specific hip geometry affects predicted hip joint contact forces during gait. J. Biomech. 41, 1243-1252.
Lu, T.-W., O'connor, J., 1999. Bone position estimation from skin marker co-ordinates using global optimisation with joint constraints. J. Biomech. 32, 129-134.
McGinley, J.L., Baker, R., Wolfe, R., Morris, M.E., 2009. The reliability of three-dimensional kinematic gait measurements: A systematic review. Gait Posture 29, 360-369.
Novacheck, T.F., 1998. The biomechanics of running. Gait Posture 7, 77-95.
O'Connor, M.K., Bottum, C.M., 2009. Differences in Cutting Knee Mechanics Based on Principal Components Analysis. Med. Sci. Sports Exerc. 41, 867-878.
Ojeda, J., Martínez-Reina, J., Mayo, J., 2016. The effect of kinematic constraints in the inverse dynamics problem in biomechanics. Multibody System Dynamics 37, 291-309.
Palisano, R., Rosenbaum, P., Bartlett, D., Livingston, M., 2007. Gross motor function classification system expanded and revised (gmfcs-e & r). CanChild Center for Childhood Disability Research, McMaster University.
Palmieri-Smith, R., McLean, S., Ashton-Miller, J., Wojtys, E., 2009. Association of Quadriceps and Hamstrings Cocontraction Patterns With Knee Joint Loading. Journal of Athletic Training 44, 256-263.
Peters, A., Galna, B., Sangeux, M., Morris, M., Baker, R., 2010. Quantification of soft tissue artifact in lower limb human motion analysis: a systematic review. Gait Posture 31, 1-8.
Potvin, B.M., Shourijeh, M.S., Smale, K.B., Benoit, D.L., 2017. A practical solution to reduce soft tissue artifact error at the knee using adaptive kinematic constraints. J. Biomech.
Robin, J., Graham, H.K., Baker, R., Selber, P., Simpson, P., Symons, S., Thomason, P., 2009. A classification system for hip disease in cerebral palsy. Dev. Med. Child Neurol. 51, 183-192.
Robinson, M.A., Donnelly, C.J., Tsao, J., Vanrenterghem, J., 2014. Impact of knee modeling approach on indicators and classification of ACL injury risk. Med. Sci. Sports Exerc. 46, 1269-1276.
Rosenbaum, P., Paneth, N., Leviton, A., Goldstein, M., Bax, M., Damiano, D., Dan, B., Jacobsson, B., 2007. A report: the definition and classification of cerebral palsy April 2006. Dev. Med. Child Neurol. Suppl. 109, 8-14.
Sangeux, M., Passmore, E., Graham, H.K., Tirosh, O., 2016. The gait standard deviation, a single measure of kinematic variability. Gait Posture 46, 194-200.
Schmitz, A., Buczek, F.L., Bruening, D., Rainbow, M.J., Cooney, K., Thelen, D., 2016. Comparison of hierarchical and six degrees-of-freedom marker sets in analyzing gait kinematics. Computer methods in biomechanics and biomedical engineering 19, 199-207.
Sheehan, F.T., Seisler, A.R., Alter, K.E., 2008. Three-dimensional in vivo quantification of knee kinematics in cerebral palsy. Clin. Orthop. Relat. Res. 466, 450-458.
Sheehan, F.T., Seisler, A.R., Siegel, K.L., 2007. In vivo talocrural and subtalar kinematics: a non-invasive 3D dynamic MRI study. Foot Ankle Int. 28, 323-335.
Smale, K.B., Potvin, B.M., Shourijeh, M.S., Benoit, D.L., 2017. Knee joint kinematics and kinetics during the hop and cut after soft tissue artifact suppression: Time to reconsider ACL injury mechanisms? J. Biomech.

Stanhope, S., Kepple, T., McGuire, D., Roman, N., 1990. Kinematic-based technique for event time determination during gait. Med. Biol. Eng. Comput. 28, 355-360.
Steinwender, G., Saraph, V., Scheiber, S., Zwick, E.B., Uitz, C., Hackl, K., 2000. Intrasubject repeatability of gait analysis data in normal and spastic children. Clin. Biomech. 15, 134-139.
Sullivan, G.M., Feinn, R., 2012. Using effect size—or why the P value is not enough. Journal of graduate medical education 4, 279-282.
Sutherland, D.H., 2002. The evolution of clinical gait analysis: Part II Kinematics. Gait Posture 16, 159-179.
Verschuren, O., Bloemen, M., Kruitwagen, C., Takken, T., 2010. Reference values for anaerobic performance and agility in ambulatory children and adolescents with cerebral palsy. Dev. Med. Child Neurol. 52, e222-e228.
Williams, D.S., Davis, I.M., Scholz, J.P., Hamill, J., Buchanan, T.S., 2004. High-arched runners exhibit increased leg stiffness compared to low-arched runners. Gait Posture 19, 263-269.
Wong, A.Y.C., Sangeux, M., Baker, R., 2010. Calculation of joint moments following foot contact across two force plates. Gait Posture 31, 292-293.
Yu, B., Gabriel, D., Noble, L., An, K.-N., 1999. Estimate of the optimum cutoff frequency for the Butterworth low-pass digital filter. J. Appl. Biomech. 15, 318-329.

Figure 1 Mean Joint Angle SDs

Figure 2 Comparison of hip, knee and ankle angles and moments from three models within a subject; mean (solid line) and standard deviation (shaded)

Figure 3 Mean Joint Moment SDs

Figure 4. Known Groups Analysis: Hedge's g Effect Sizes

Table 1: Marker Set

SEGMENT	ABBREVIATION	PLACEMENT/FULL NAME	Anatomical	Tracking
Foot	RMT1, LMT1	Right/Left 1st metatarsal head	✓	✓
	RMT5, LMT5	Right/Left 5th metatarsal head	✓	✓
	RCAL, LCAL	Right/Left calcaneus (middle of posterior aspect)	✓	✓
Shank/leg	RMMAL, LMMAL	Distal end of tibia, medial malleolus	✓	
	RLMAL, LLMAL	Distal end of fibula, lateral malleolus	✓	
	RTB1, LTB1 RTB2, LTB2 RTB3, LTB3	Right/Left Tibia: Long bar runs along tibia axis and the short bar wraps laterally.		✓
Thigh	RMFC, LMFC	Right/Left Medial Femoral Condyle	✓	
	RLFC, LLFC	Right/Left Lateral Femoral Condyle	✓	
	RTH1, LTH1 RTH2, LTH2 RTH3, LTH3	Right/Left Thigh: Long bar runs along Iliotibial band and short bar wraps anteriorly		✓
Pelvis	RASI, LASI	Right/Left Anterior Superior Iliac Spine	✓	✓
	RPSI, LPSI	Right/Left Posterior Superior Iliac Spine	✓	✓

Table 2: IK Models

Model	POSE filter frequency	Optimizer	Segment	Weight factor	Translations	Translation Constraints (proximal end of distal segment with respect to distal end of proximal segment)				Model Performance (Translation mean (SD))			
IK3	6Hz	Levenberg Marquardt: default in Visual 3D™	Pelvis RTH RSK RFT	4 2 3 4	X Y Z 0 0 0 0 0 0 0 0 0								
IK6	6Hz	Levenberg Marquardt	Pelvis RTH RSK RFT	4 2 3 4	X Y Z X Y Z X Y Z X Y Z	None				Hip Knee Ankle	X Y Z X Y Z X Y Z	-17mm(17mm) -24mm(32mm) -20mm(21mm) -11mm(17mm) -7mm(13mm) -31mm(15mm) -7mm(8mm) -10mm(9mm) -11mm(9mm)	20mm(22mm) 21mm(15mm) 17mm(12mm) 9mm(12mm) 15mm(21mm) 1mm(14mm) 4mm(8mm) 4mm(9mm) 0mm(5mm)
IK6C	6Hz	LBFGSB: uses an estimation to the inverse Hessian matrix for optimizing variables subject to simple bounds[1]. It is more time consuming than the Levenberg Marquardt optimizer.	Pelvis RTH RSK RFT	4 2 3 4	X Y Z X Y Z X Y Z X Y Z	Hip Knee Ankle	X Y Z X Y Z X Y Z	-5mm (lateral) -5mm (posterior) -5mm (inferior) -15mm (lateral) -15mm (posterior) -20mm (inferior) -5mm (lateral) -6mm (anterior) -3mm (inferior)	5mm (medial) 5mm (anterior) 5mm (superior) 10mm (medial) 15mm (anterior) 0mm (superior) 3mm (medial) 4mm (anterior) 5mm (superior)	Hip Knee Ankle	X Y Z X Y Z X Y Z	-5mm(1mm) -5mm(1mm) -5mm(2mm) -10mm(4mm) -15mm(2mm) -20mm(7mm) -4mm(1mm) -6mm(1mm) -2mm(6mm)	5mm(1mm) 6mm(1mm) 6mm(2mm) 10mm(4mm) 12mm(5mm) -4mm(5mm) 4mm(1mm) 4mm(1mm) 2mm(2mm)

Hz=Hertz; IK3=three degree of freedom inverse kinematic model; IK6=six degree of freedom inverse kinematic model; IK6C= six degree of freedom inverse kinematic model with specified joint constraint boundaries; LBFGSB= Limited-memory Broyden-Fletcher–Goldfarb–Shanno; mm=millimeters; POSE= Position and Orientation of a Segment; RTH=Right Thigh; RSK=Right Shank; RFT=Right Foot; SD=Standard Deviation;

[1] Zhu C, Byrd RH, Lu P, Nocedal J. Algorithm 778: L-BFGS-B: Fortran subroutines for large-scale bound-constrained optimization. ACM Trans Math Softw. 1997;23:550-60.

Highlights

- A 6DoF biomechanical model with customised joint constraints is described
- Customised joint translation constraints decrease extrinsic variability
- This results in a larger effect size for hip power generation in swing

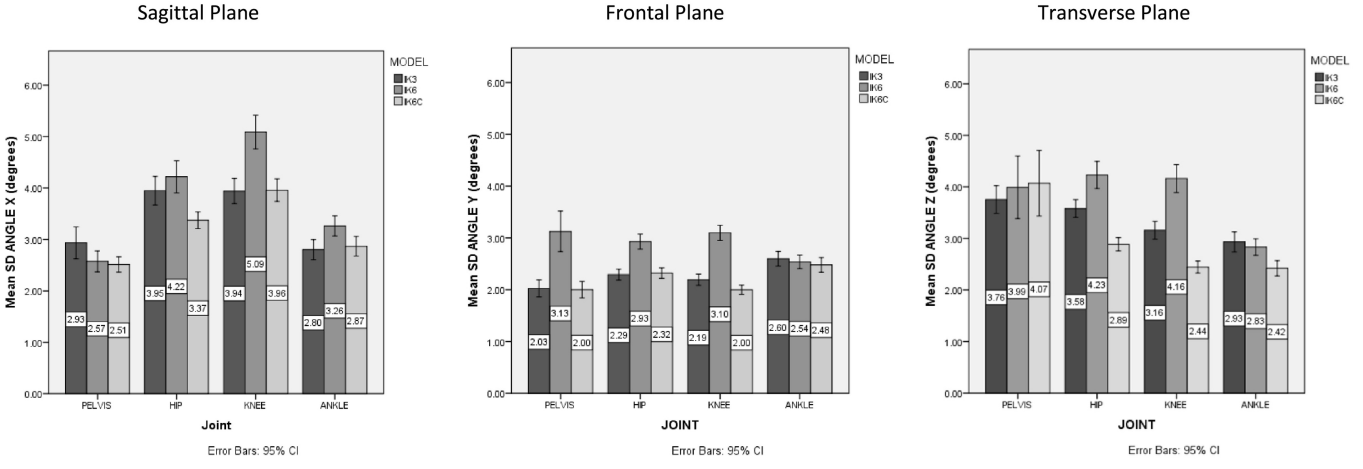

SD=standard deviation, CI=confidence interval, IK6C=IK6Constrained model

Figure 1

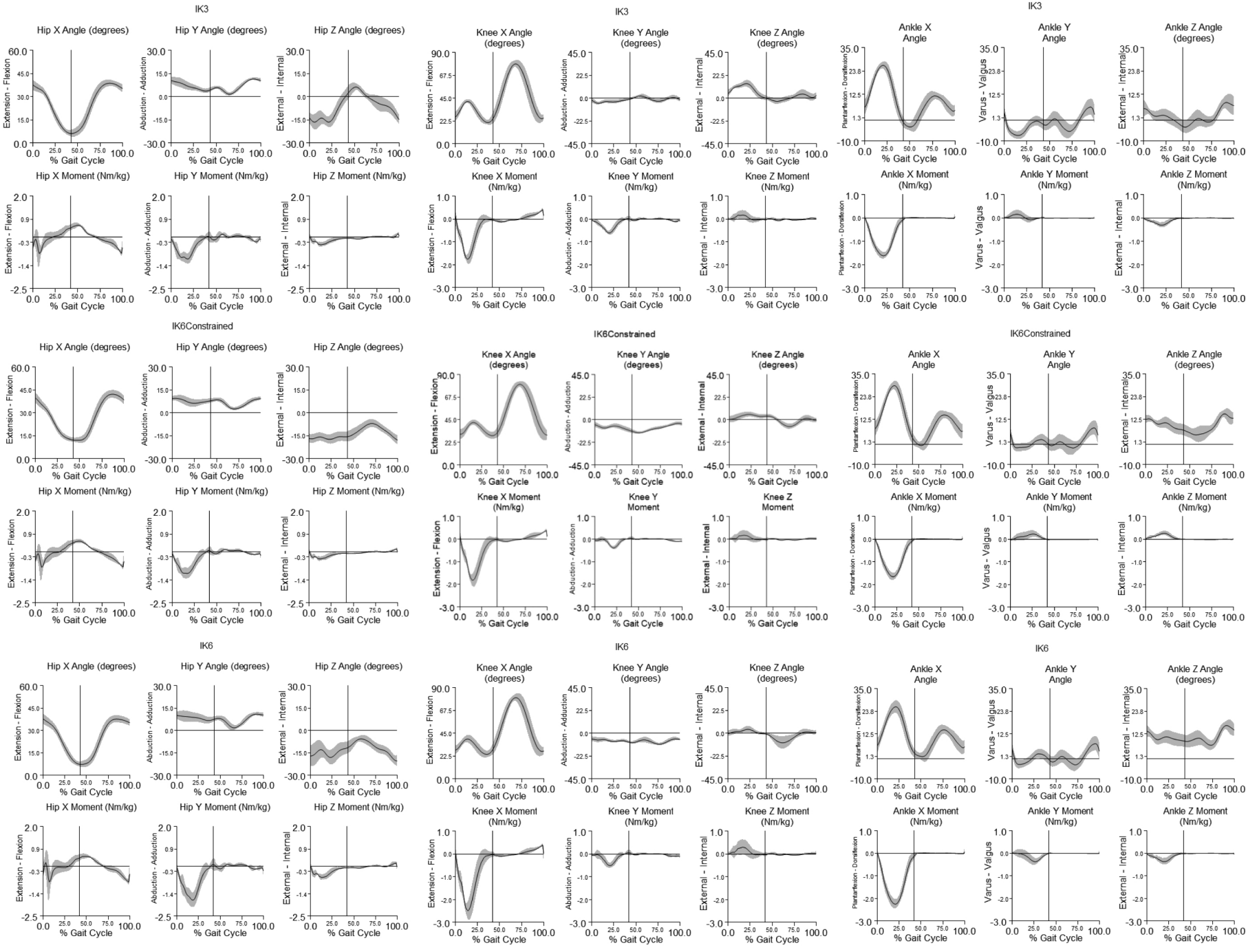
IK3
Hip X Angle (degrees)
Hip Y Angle (degrees)
Hip Z Angle (degrees)
Hip X Moment (Nm/kg)
Hip Y Moment (Nm/kg)
Hip Z Moment (Nm/kg)
Knee X Angle (degrees)
Knee Y Angle (degrees)
Knee Z Angle (degrees)
Knee X Moment (Nm/kg)
Knee Y Moment (Nm/kg)
Knee Z Moment (Nm/kg)
Ankle X Angle
Ankle Y Angle
Ankle Z Angle (degrees)
Ankle X Moment (Nm/kg)
Ankle Y Moment (Nm/kg)
Ankle Z Moment (Nm/kg)
IK6Constrained
IK6
Extension - Flexion
Abduction - Adduction
External - Internal
Plantarflexion - Dorsiflexion
Varus - Valgus
% Gait Cycle

Figure 2

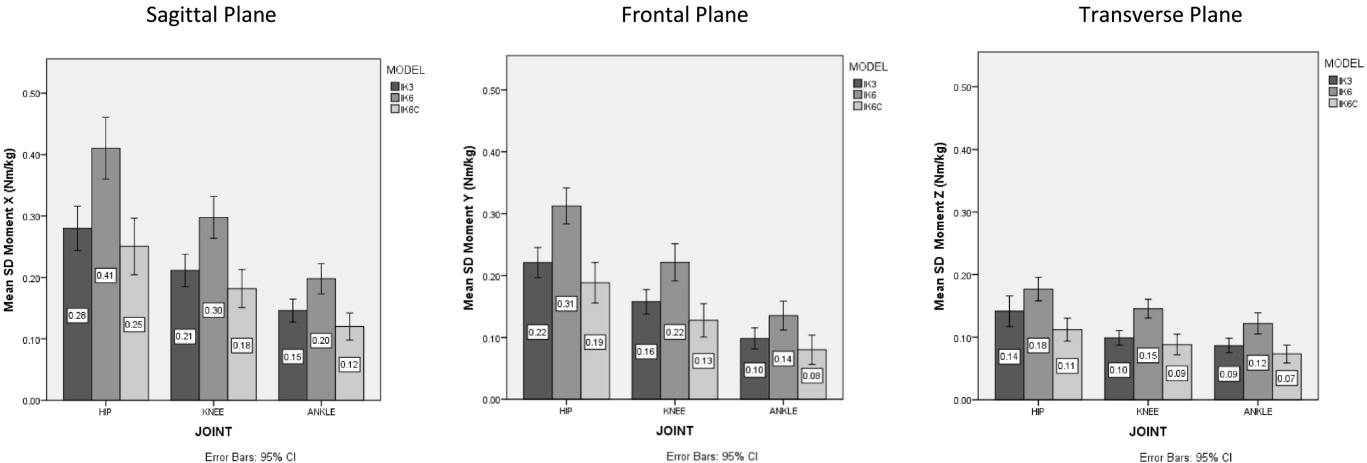

SD=Standard deviation, Nm/kg=Newton metres per kilogram, CI=confidence interval, IK6C=IK6Constrained model

Figure 3

Known Groups Analysis: Hedge’s g Effect Sizes

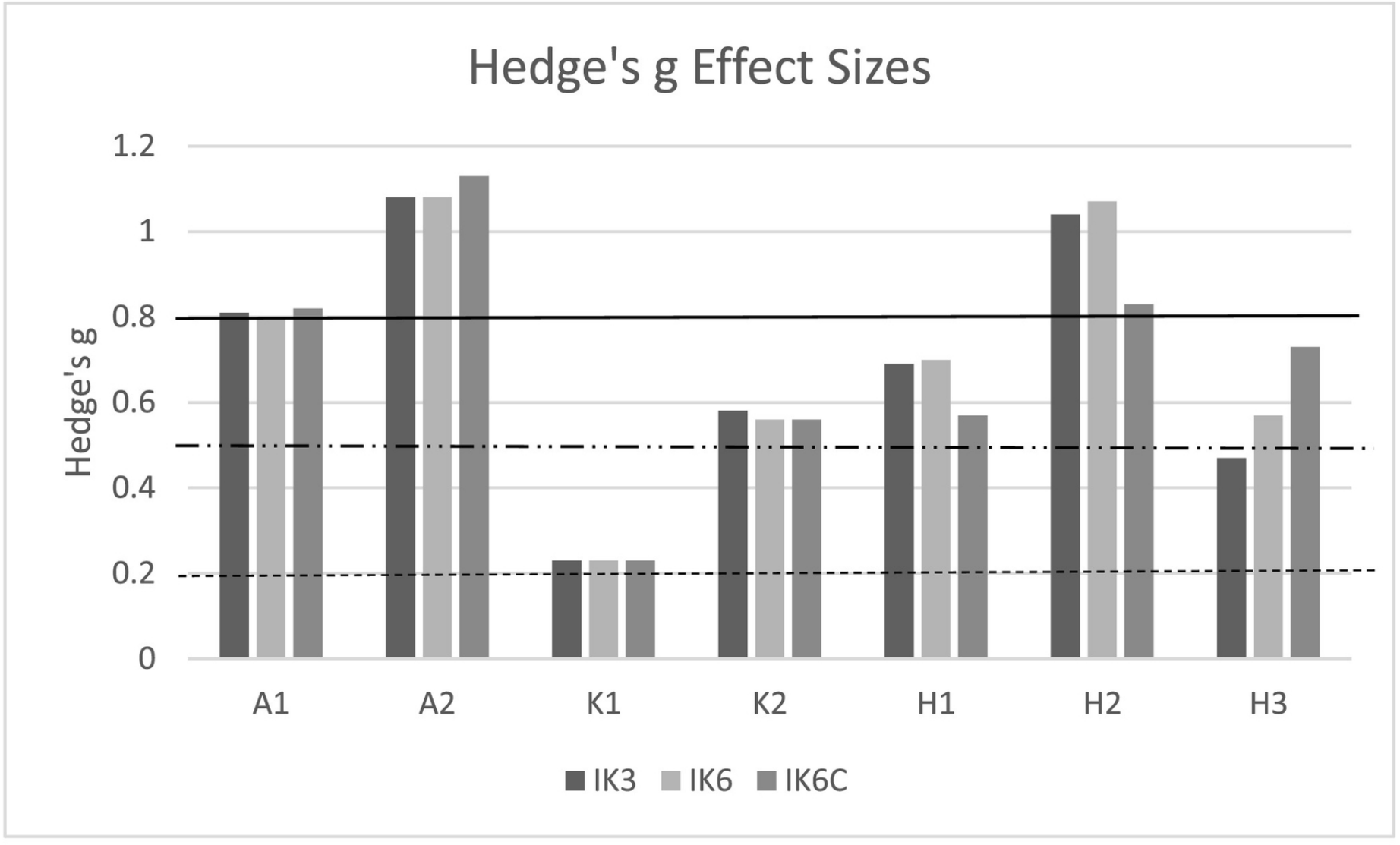

Figure 4